H^+-H^- coincidences from the three-body dissociation of excited H_3^+

O. Yenen, D. Calabrese, L. M. Wiese, and D. H. Jaecks
Behlen Laboratory of Physics, University of Nebraska, Lincoln, Nebraska 68588-0111

Gordon A. Gallup
Department of Chemistry, University of Nebraska, Lincoln, Nebraska 68588-0304
(Received 7 May 1992)

The laboratory energy distribution of protons in coincidence with an H^- ion, resulting from the dissociation of excited H_3^+, has been measured for H^+-H^- pairs emitted along the beam for 4.0-keV H_3^+-He collisions. An approximate energy distribution of H^+-H^- pairs for the collinear configuration of the dissociation products is obtained by transforming the measured laboratory spectrum to the H_3^+ center-of-mass (c.m.) frame. Coincidence data suggest that the reaction producing H^+-H^- pairs where the H^+ ion has near-zero energies (<0.5 eV) in the c.m. frame is a low-probability process. We have also computed the adiabatic Born-Oppenheimer energies of H_3^+ ions using a full configuration-interaction calculation with a basis set of atomic orbitals consisting of $1s$, $1s'$, $1p'$, $2s$, and $2p$ centered on the protons forming an isosceles (C_{2v} symmetry) or an equilateral (D_{3h} symmetry) triangle. The states leading to asymptotic $H^+ + H^+ + H^-$ limits have been identified by calculating $\langle 1/r_{12} \rangle^{-1}$, the inverse of the expectation value of the electron-electron repulsion term. The states identified by this procedure have adiabatic Born-Oppenheimer energies of 40–45 eV above the H_3^+ ground state at the H_3^+ equilibrium separation. The limits on the total available internal energy to be shared by the three dissociation products that one obtains from the experimentally determined H^+-H^- coincidence spectrum are consistent with the identified H_3^+ excited states.

PACS number(s): 34.50.Gb

I. INTRODUCTION

A complete understanding of the general three-body problem is of fundamental importance for all branches of physics. Of particular interest is the Coulomb three-body problem where the interaction among the particles is dominated by the long-range Coulomb potential. The escape of two electrons from an atom after electron impact near the threshold of ionization, the photodetachment of two electrons from a negative ion, or the breakup of a molecular ion into three fragments where one of the fragments has the opposite charge of the other two, are classical examples of three-body Coulomb problem.

The theoretical development of the three-body Coulomb problem was started by the classical theory of Wannier [1]. These results were reformulated by Peterkop [2] and independently by Rau [3] using semiclassical methods. Klar [4], using hyperspherical coordinates, extended the theory to include three-body systems of arbitrary mass having total angular momentum $L=0$. Feagin [5] further developed the theory within the WKB approximation for arbitrary mass and for $L>0$. The Wannier technique was also applied to the calculation of the sharing of the available potential energy by the like charges [6,7], and the distribution of the correlation angle between the like charges [8].

To date, almost all experimental studies to verify the predictions of the theory have concentrated on the study of systems where two electrons escape from a massive nucleus. Most of the experimental studies focused on the energy dependence of the total electron-impact ionization cross sections near the threshold of ionization [9]. More recently, the predictions of the Wannier theory for the distribution of the correlation angle θ_{12} between the two electrons were experimentally verified for double photoionization [10]. It is obvious, however, that a system consisting of two electrons and a nucleus cannot probe any mass-dependent effects of the theory, and a complete test requires that measurements on massive particles be carried out. In addition, in the case of two electrons nearly all the energy is carried away by the two electrons. In a system of nearly equal masses the energy sharing is more democratic. Unfortunately, the experimental difficulties associated with most ideal systems, such as the slow-moving $\bar{p}+p+p$ or $p+\mu^-+\pi^+$, are overwhelming.

The three-body decay of excited H_3^+ into $H^+ + H^- + H^+$ appears to be the most viable candidate for the study of different aspects of the three-body Coulomb problem for equal-mass particles [11,4]. To date, we have reported measurements of the laboratory and center-of-mass (c.m.) energy distributions of H^- produced in 4.0-keV H_3^+-He collisions at 0° with respect to the beam direction [11]. We have also measured the laboratory and c.m. energy distributions of protons [12], though there are many more channels that produce H^+ from H_3^+ than produce H^-. In this paper, we report on the measurement of the laboratory energy distribution of protons which are in coincidence with a H^- that results from the dissociation of a beam of excited H_3^+ formed in 4.0-keV H_3^+-He collisions. The measurements are carried out for the case when both H^+ and H^- are emitted nearly parallel to the incoming beam direction. This ex-

perimental layout provides information about the collinear dissociation of $(H_3^+)^*$ into $H^+ + H^+ + H^-$. In addition, as we will see, the range of total internal energies available for all three particles in the c.m. frame for dissociating H_3^+ can be estimated from our data. We also present the results of configuration-interaction (CI) calculations for the energies as a function of the separation between the protons of the dissociative states producing asymptotically $H^+ + H^+ + H^-$ in both D_{3h} and C_{2v} symmetries.

II. EXPERIMENTAL PROCEDURE AND RESULTS

The apparatus used in these measurements has been described in our previous work [12,14]. H_3^+ ions from a duoplasmatron source are accelerated to 4.0 keV, mass selected by an analyzing magnet, and focused. Subsequently, the H_3^+ beam collides under single-collision conditions with the He target gas in a differentially pumped, 1-cm-long cell. The dissociation products proceed to a three-parallel-plate electrostatic energy analyzer which separates the positive and negative ions as shown in Fig. 1. Using microchannel plates (MCP's), the protons are detected at $0.000° \pm 0.024°$ relative to the beam direction with a full width at half maximum (FWHM) energy resolution of 0.33%. Again using MCP's, H^- ions are detected at $0.00° \pm 0.25°$ with respect to the incoming beam direction. We also measured the Ly-α photon counts resulting from any H(2p) as well as near Ly-α radiation resulting from excited H_2 formed from collisions inside the cell. These were used for normalization purposes, since the photon count rate is proportional to the target-density–beam-current product.

Single pulses from each detector, after amplification, discrimination, and appropriate delays, are fed into a time-to-amplitude converter (TAC). We used the H^- signal as the "start," and the proton signal as the "stop" input of the TAC. The output of the TAC is connected to a multichannel analyzer (MCA) in its pulse-height-analysis mode. Coincidences are accumulated for a chosen voltage of the energy analyzer, which in turn fixes the laboratory energy of the proton. At the end of a run, the data are transferred into a computer for further data reduction and analysis, the voltage of the energy analyzer is then set to a new value, and the procedure repeated. Thus, for each laboratory energy of the proton, we obtained a coincidence spectrum between a proton of fixed energy and a H^-, when both are emitted parallel to the beam direction. We found no coincidences between H^+ and H^- from H_3^+ when the collision cell was at the background gas pressure of 5×10^{-8} Torr. This approach eliminates the possibility of H^+-H^- coincidences originating from metastable $(H_3^+)^*$ ions or from scattering of H_3^+ from slits or apertures.

From time spectra, we determined the integrated number of true coincidences for the selected H^+ laboratory energies. In Fig. 2, the number of true coincidences is shown as a function of the laboratory energy of the proton. The error bars denote the statistical errors in evaluating the true coincidences. Also shown in Fig. 2 is the total H^+ laboratory energy spectrum resulting from all processes. The central peak of the total H^+ spectrum corresponds to particles having near-zero energies in the center-of-mass (c.m.) frame of H_3^+ [13]. With negligible transverse velocities, the ions at this peak move along with the beam and are collected with high efficiency, yet the coincidence spectrum shows there are very few protons of zero energy that are simultaneously formed with H^-. This is what we would expect for the breakup of three particles when the three particles lie along or near the beam axis with the H^- between the two protons. The limited range of acceptance angle of the detectors means that we are not seeing all possible coincidences; in particular, protons or H^- with large transverse velocities with respect to the beam direction do not reach the detectors. Assuming an isotropic distribution of emitted protons in the c.m. frame of H_3^+, it is possible to approximately correct for the proton detector's solid angle [13]. Data corrected for the solid angle effects of the H^+ detector are presented in Fig. 3. The vertical marks in Fig. 3 denote the H^+ energies in the c.m. frame of H_3^+. These values do not increase linearly, a result of the properties of the transformation equations from the laboratory

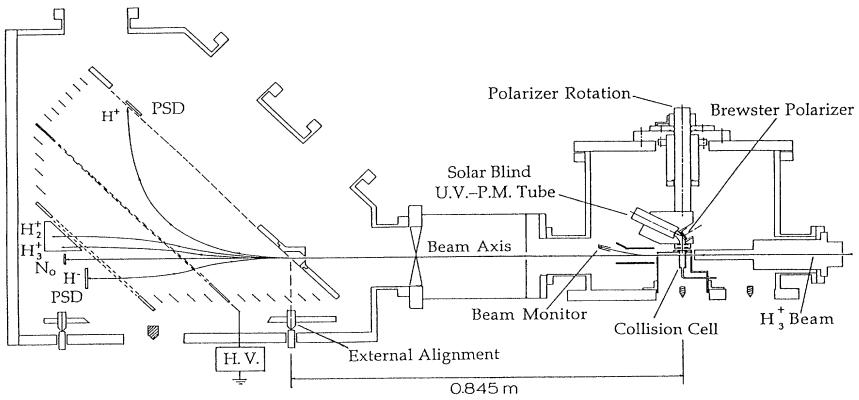

FIG. 1. Schematic view of the energy analyzer and the detectors. PSD denotes a position-sensitive detector, HV denotes a high-voltage supply, and PM denotes a photomultiplier tube.

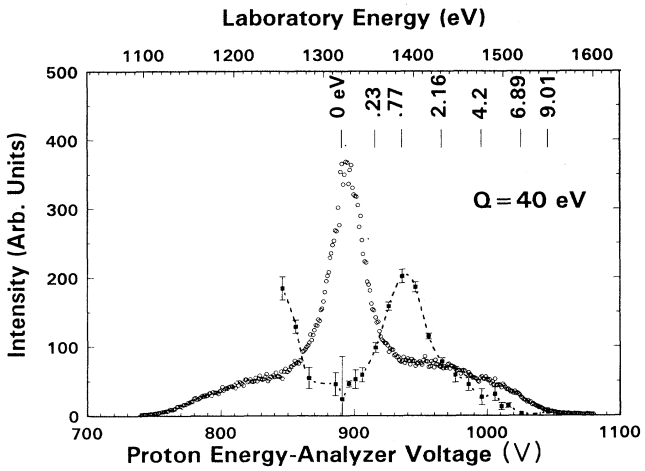

FIG. 2. Integrated number of true coincidences (solid squares) as a function of the laboratory energy (top scale) of the protons. The bottom scale shows the corresponding voltage of the parallel-plate analyzer. The true coincidences are normalized to the Ly-α counts. Also shown is the total laboratory energy distribution of protons (open circles). The error bars denote the statistical errors associated with the coincidence measurements. The dashed line is a cubic-spline interpolation to guide the eye. The vertical lines show representative center-of-mass energies of the protons. One should note that there are no H$^+$-H$^-$ coincidences for near-zero center-of-mass-energy protons.

frame to the c.m. frame. We also want to emphasize that the distribution of Fig. 3 does not represent all possible three-body states that can result in the formation of $H^+ + H^+ + H^-$, due to the restriction that the H$^+$-H$^-$ pairs are nearly collinear in the laboratory.

The center of symmetry of the dip in the coincidence

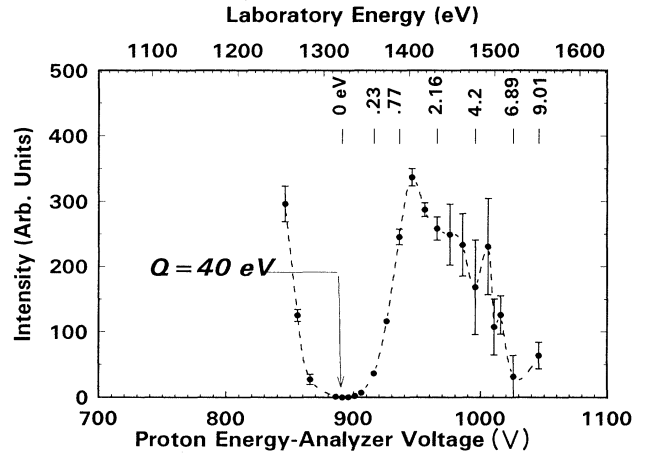

FIG. 3. Integrated number of true coincidences as a function of the laboratory energy (top scale) of the protons, corrected for the solid angle effects of the proton detector. The bottom scale shows the corresponding voltage of the parallel plate analyzer. As in Fig. 2, the vertical lines show representative center-of-mass energies of the protons. The error bars denote the statistical errors associated with the coincidence measurements. The dashed line is a cubic-spline interpolation to guide the eye.

data of Fig. 3 determines the laboratory energy of protons that have zero energy in the c.m. frame of H_3^+. Protons with laboratory energies larger than this amount move forward in the c.m. frame of H_3^+, in the same direction as the initial beam. Protons with energies less than the center of symmetry of the dip move in a direction opposed to the direction of the incoming beam. The laboratory energy of the center of the dip corresponds to a laboratory energy of $(E_0 - Q)/3$, where E_0 is the energy of the incoming beam and Q is the inelastic energy loss associated with protons that have zero velocity in the c.m. frame of H_3^+.

This inelastic energy loss is determined by adjusting the value of Q until c.m. coincidence energy distributions are symmetric for protons moving forward or backward in the c.m. frame of the dissociating H_3^+. From coincidence data we determine Q to be 40 eV. This value of Q is used in the transformation of the energy distribution of H$^+$-H$^-$ pairs from the laboratory frame to the c.m. frame. This procedure is approximate since in reality we have a distribution of Q's. Yet, this approximation does not considerably affect our results since the transformation equations are relatively insensitive to the value of Q. In fact, changing Q from 40 to 30 eV introduces only an approximate shift in the c.m. energies of 0.2 eV.

The value of Q is different from our original value of 60 eV, published in Ref. [12], that we used for the transformation of H$^-$ energies from the laboratory coordinate system to the H_3^+ c.m. frame. This larger number for the inelastic energy loss in our original published work [12] resulted from the fact that the original calibration procedure for our parallel-plate energy analyzer led to large uncertainties in the measured energies. We recalibrated the energy analyzer using the minor trace ions present in the ion source as well as defocused beams of H$^+$, H_2^+, and H_3^+. In this procedure, we related the voltage of the analyzer to the potential applied to the ion source when the beam hit the detector. The resulting analyzer constant is used to determine the energy of ions at arbitrary voltages. This procedure automatically reduces to negligible values any errors in the measured proton energies associated with energy shifts [15] inside the ion source. This new method of calibration was also used for the dissociation studies of H_2^+-He collisions [16].

III. CALCULATION OF H_3^+ ENERGIES

The energy distribution of H$^+$-H$^-$ pairs we experimentally determined must be consistent with the potential-energy curves of H_3^+. Although the excited states of H_3^+ were previously calculated [17,18], the excited states leading to the production of $H^+ + H^+ + H^-$ have never been identified. In this section, in addition to the calculation of the excited states, a novel method to identify the excited states leading asymptotically to $H^+ + H^+ + H^-$ is presented.

A linear combination of atomic orbitals (LCAO) full configuration-interaction (CI) calculation of the adiabatic energies was carried out for H_3^+ in a number of equilateral triangle and isosceles triangle geometries. The basis

TABLE I. Coefficients of the Gaussian basis for H_3^+. The coefficients α_i are the exponents and C_i are the scale coefficients. A set like this is centered at each nucleus.

Type	α_i	C_i
1s (short range)[a]	68.16	0.002 55
	10.246 5	0.019 38
	2.346 48	0.092 80
	0.673 320	0.294 30
	0.224 660	0.492 21
1s′ (long range)[a]	0.082 217	1.000 00
1p′	1.1	1.000 00
2s[a]	0.984 13	−0.053 85
	0.037 634	0.603 35
	0.014 660	0.444 92
2p[a]	0.337 072	0.092 05
	0.079 830	0.474 06
	0.024 684	0.578 60

[a]Taken from Ref. [20].

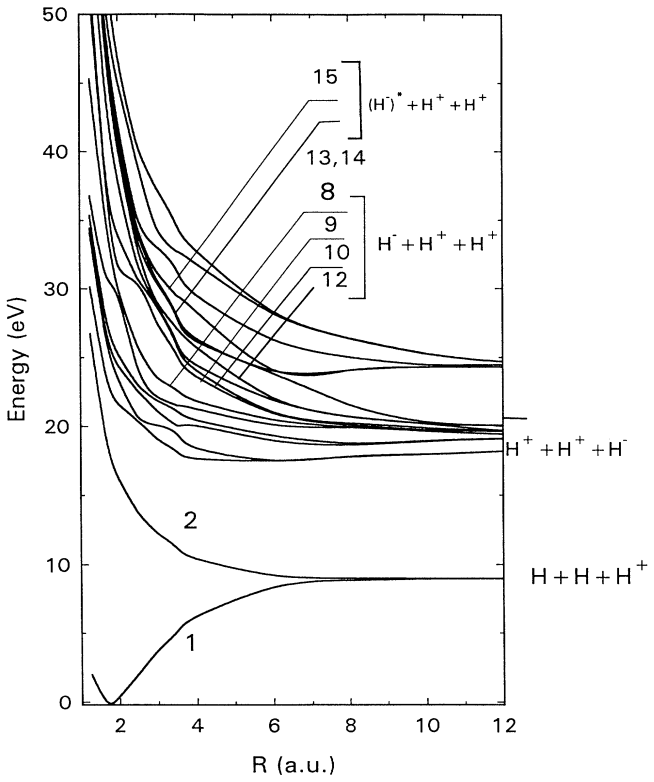

FIG. 4. The adiabatic Born-Oppenheimer energies of the first 18 $^1A_1'$ and $^1E_1'$ states of H_3^+ calculated as described in the text for the D_{3h} symmetry (equilateral triangle). R is the equilateral triangle's edge. The numbers next to the curves refer to the ascending ordering of the states at the equilibrium separation starting with the ground state. Only the curves 8, 9, 10, and 12 can produce a ground-state H^-; states 13–15 produce an excited $(H^-)^*$ which autoionizes.

of atomic orbitals (AO's) at each H-atom center was 1s, 1s′, 1p′, 2s, and 2p, for a total of 9 AO's. This produces a total of 27 molecular orbitals (MO's) and, from the Weyl dimension formula [19], a total of 378 two-electron singlet functions. We restrict our interest to singlet functions since the triplet states of H_3^+ cannot dissociate into a stable H^- without a spin flip. The coefficients of the Gaussian basis are based on the set given by Huzinaga [20] and are presented in Table I.

The equilateral triangle states of the ion possess D_{3h} symmetry. The 378 two-electron singlet functions support a representation of D_{3h} that is equivalent to $52\,^1A_1' + 32\,^1A_2' + 84\,^1E' + 18\,^1A_1'' P + 24\,^1A_2'' + 42\,^1E''$. These numbers can be determined easily from tables already given by one of us [21]. Of these, only the $^1A_1'$ and the $^1E'$ states can lead to H^- ions. In Fig. 4 we show, as a function of the length of an edge of the equilateral triangle, the lowest 18 of these $^1A_1'$ and $^1E'$ energies intermixed. The $^1E'$ states are doubly degenerate.

The isosceles triangle geometries of H_3^+ possess C_{2v} (molecule in the y-z plane) symmetry and are mostly of the obtuse sort. The only exceptions are the two smallest structures, where we calculated one acute geometry and the equilateral one. The 378 two-electron singlet functions support a representation in this case equivalent to $136\,^1A_1 + 60\,^1A_2 + 66\,^1B_1 + 116\,^1B_2$. In this case only the $^1A_1$ and $^1B_2$ states can lead to stable H^- ions. In Fig. 5

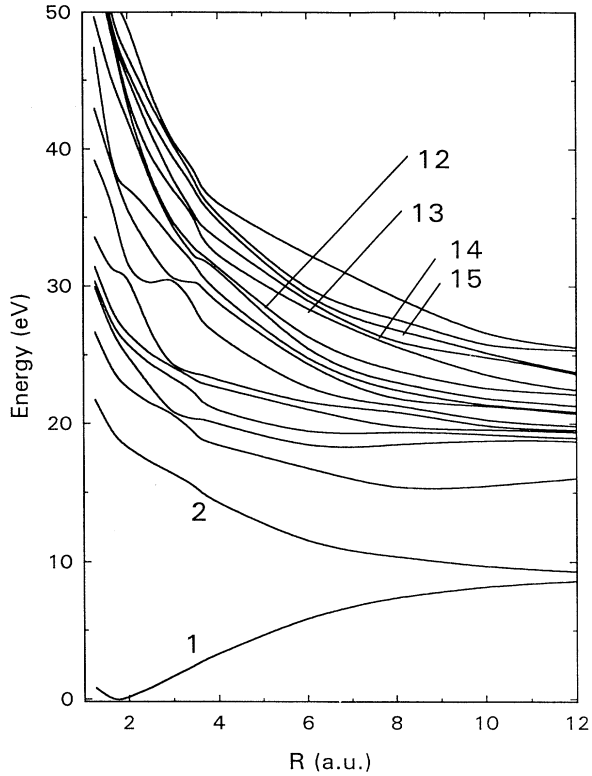

FIG. 5. The adiabatic Born-Oppenheimer energies of the first 17 $^1A_1$ states of H_3^+ calculated as described in the text for the C_{2v} symmetry (isosceles triangle). R is the length of the base of the isosceles triangle. Only the states labeled 12–15 lead to the production of two protons and a stable H^-.

we show the 17 lowest $^1A_1$ energies and in Fig. 6 we show the 18 lowest $^1B_2$ energies. In both cases these are plotted as a function of the length of the base of the isosceles triangle. The altitude of the triangle is kept fixed for all of these geometries at the equilibrium value associated with the ground-state equilateral triangle.

In order to identify the states of H_3^+ that can lead to $H^+ + H^+ + H^-$, we have also calculated the inverse of the electron-electron repulsion energy in the system, $\langle 1/r_{12} \rangle^{-1}$. In the Born-Oppenheimer approximation the total energy may be written as

$$E_{\text{tot}} = E_{\text{nuc}} + \langle T \rangle + \langle V \rangle + \langle 1/r_{12} \rangle \ ,$$

where E_{nuc} is the repulsion energy of the three protons, T is the electronic kinetic-energy term, V is the electron-proton attraction terms, and the last term is the electron-electron repulsion energy. Therefore, we have

$$\langle 1/r_{12} \rangle^{-1} = [E_{\text{tot}} - E_{\text{nuc}} - \langle T \rangle - \langle V \rangle]^{-1} \ .$$

If a state has the asymptotic form $H + H + H^+$, the expectation value of $\langle 1/r_{12} \rangle^{-1}$ should eventually increase with the size of the triangle at a rate proportional to the size. On the other hand, if the asymptotic state is $H^+ + H^+ + H^-$, $\langle 1/r_{12} \rangle^{-1}$ should be nearly independent of the size of the triangle. The graphs of $\langle 1/r_{12} \rangle^{-1}$ for selected states of the D_{3h} and C_{2v} geometries of H_3^+ are presented in Figs. 7–9, where the integers correspond to

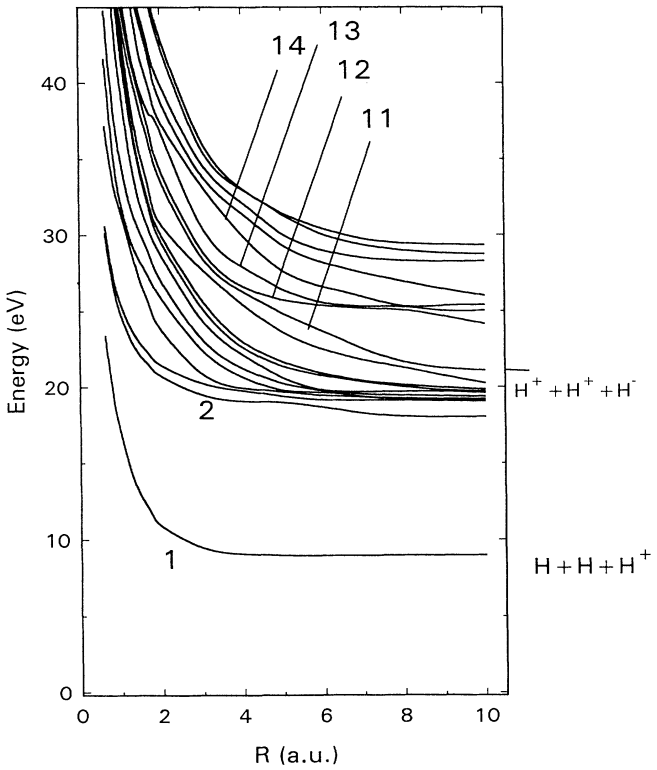

FIG. 6. The adiabatic Born-Oppenheimer energies of the first 18 $^1B_2$ states of H_3^+ calculated as described in the text for the C_{2v} symmetry (isosceles triangle). R is the length of the base of the isosceles triangle. Only the states labeled 11–14 lead to the production of two protons and a stable H^-.

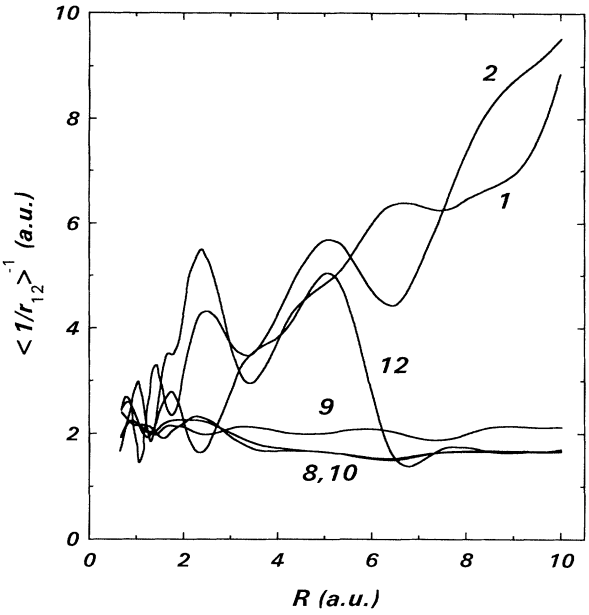

FIG. 7. The inverse of the expectation value of the electron-electron repulsion term, i.e., $\langle 1/r_{12} \rangle^{-1}$ as a function of the distance between the protons for the selected $^1A_1'$ and $^1E'$ energies of the D_{3h} configuration. The numbers refer to the ascending ordering of the corresponding energy curves in Fig. 4. Note that only the states 8, 9, 10, and 12 produce two protons and a stable H^-.

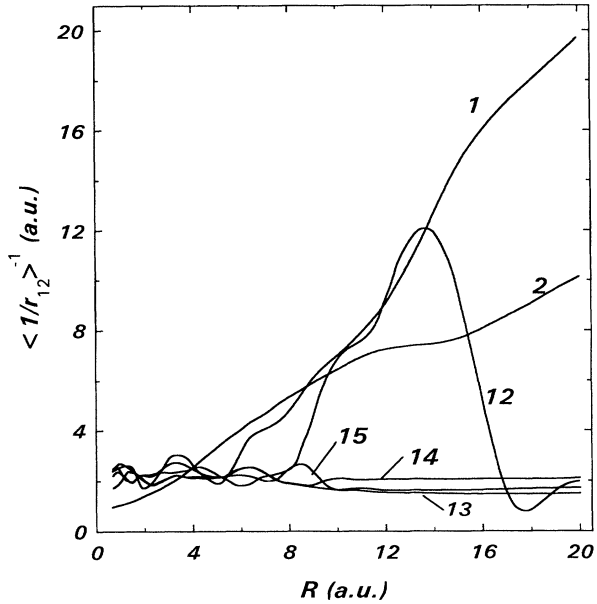

FIG. 8. The inverse of the expectation value of the electron-electron repulsion term, i.e., $\langle 1/r_{12} \rangle^{-1}$ as a function of the length of the base of the isosceles triangle, for the $^1A_1$ states of the C_{2v} configuration. The numbers refer to the ascending ordering of the corresponding energy curves in Fig. 5. Note that only the states 12–15 (inclusive) produce two protons and a stable H^-.

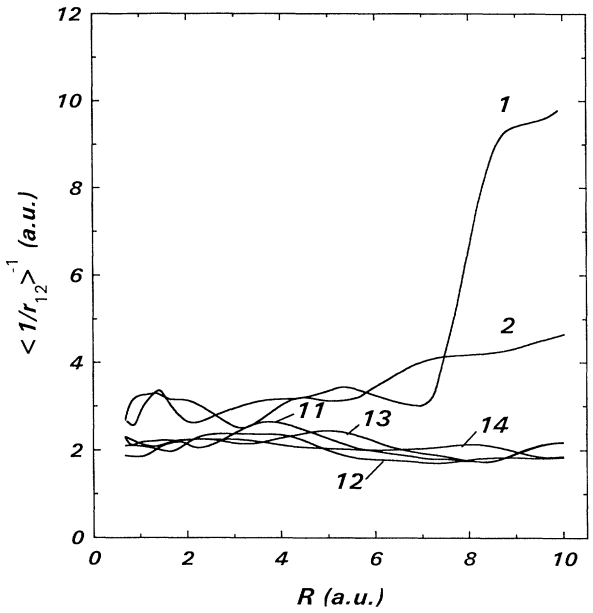

FIG. 9. The inverse of the expectation value of the electron-electron repulsion term, i.e., $\langle 1/r_{12} \rangle^{-1}$ as a function of the length of the base of the isosceles triangle, for the $^1B_2$ states of the C_{2v} configuration. The numbers refer to the ascending ordering of the corresponding energy curves in Fig. 6. Note that only the states 11–14 (inclusive) produce two protons and a stable H^-.

the ordering of the corresponding energies presented in Figs. 4–6. We show, in particular, the behavior of $\langle 1/r_{12} \rangle^{-1}$ for the two lowest-lying energy states and for those that dissociate into two protons and a stable H^- ion. We particularly note this last case, since some of the calculated states in this system represent excited H^- that are bound states only because of the relative nearness of the other protons. Such states eventually autoionize to an $H+e^-$ when the triangle becomes large enough and do not lead to states of interest in this study.

In all cases, around the equilibrium geometry of H_3^+, the energies of the adiabatic states that asymptotically go to $H^+ + H^+ + H^-$ have values in the range 40–45 eV above the ground state at the equilibrium separation of H_3^+.

There are, of course, states of H with $n > 2$ whose energies intervene between the energies of $H^+ + H + H$ and $H^+ + H^+ + H^-$ asymptotic states. These should be included in a complete treatment of this system. Nevertheless, we feel that the inclusion of the $n = 2$ states gives a representative behavior of nonvalence states in this process. In this connection we observe that the states for $n = 3, 4, \ldots$ are even more diffuse than those for $n = 2$ and are expected to interact less with valencelike states than do the $n = 2$ ones. They should therefore have less influence on these processes.

IV. DISCUSSION AND CONCLUSIONS

In this paper we have presented a measurement of the energy distribution of protons in coincidence with a H^- for the collinear configurations of the three-body system (Fig. 1). Transforming this laboratory energy distribution we obtain the approximate energy distribution of H^+ found to be in coincidence with H^-, in the H_3^+ c.m. frame (Fig. 2). We emphasize that this distribution is for the near-collinear configuration of the dissociation products, due to the experimental configuration of the apparatus.

Although detailed information about the dynamical configuration of the $H^+ + H^+ + H^-$ three-body system can only be found by measuring the laboratory energies and angles of the three particles in coincidence, we can show that our present measurements are consistent with the theoretical calculations of the H_3^+ energy states leading asymptotically to $H^+ + H^+ + H^-$, also presented in this paper. To do this, we use the former measurements of the c.m. energy distribution of H^- obtained in a noncoincidence experiment [12]. These earlier results show that the H^- distribution in the H_3^+ c.m. frame has a broad maximum at about 0.75 eV with the distribution extending out to 2.5–3 eV. Although this spectrum does not exhibit a sharp cutoff at around 2.5–3.0 eV, the distribution beyond this region is small. We also use the fact that our present coincidence data show a H^+ distribution in the c.m. frame of H_3^+ that is largest from about 0.75 to 4 eV. As discussed earlier, a distribution of inelastic energy losses are most likely and our transformed distribution is approximate.

The range of total internal energies available for the three particles can be estimated from our present coincidence data and our previously measured H^- distribution [12]. By taking various colinear combinations of H^+ energies from 0.75 to 4 eV, and H^- energies from zero to 3 eV, we calculate the c.m. energy of the third, undetected H^+ using the conservation of energy and momentum. The sum of these energies in turn gives the total internal energy available for the colinear dissociation process. This available energy ε_t varies from about 1.5 eV up to 18 eV. We see that the distribution of a H^+ coincident with a H^- with c.m. energies from 0.75 to 4 eV can result from a colinear process with a wide range of total internal energy ε_t. This wide variability is characteristic of the three-body decay in that energy and momentum conservation are not sufficient to determine the total available internal energy uniquely.

The range of ε_t is consistent with our calculated total internal energy of the excited H_3^+ states that asymptotically produce $H^+ + H^+ + H^-$. The total internal energy ε_t in Fig. 4 corresponds to the energy difference between the potential energy of the excited state at a given internuclear separation, and the $H^+ + H^+ + H^-$ asymptotic limit. The ε_t range of 1.5–18 eV, determined from the coincidence data as explained above, is compatible with the energies one would obtain from the identified potential curves of Fig. 4.

We also found essentially no H^+ of zero c.m. energy in coincidence with H^-. This implies that the configurations where a proton with zero energy, and a H^+ and a H^- go off back-to-back in the c.m. of H_3^+, while carrying away the available energy, is unlikely, since the energy and momentum are conserved in the

c.m. of the dissociating H_3^+.

In conclusion, the observed $H^+ - H^-$ coincidence distribution results from the excitation of H_3^+ to the states not previously theoretically identified. After the excitation which occurs in D_{3h} symmetry, the dissociation may proceed through different geometries to the final $H^+ + H^+ + H^-$ asymptote. The present experiment probed only the collinear configuration. These results are needed in designing the more complete triple-coincidence experiments to test the angular correlations for the three-body Coulomb problem.

ACKNOWLEDGMENTS

We thank Dr. J. R. Peterson of Stanford Research Institute for discussions about the energy-calibration procedures. The support of this work in part by the National Science Foundation under Grant No. 9119818 is gratefully acknowledged.

[1] G. H. Wannier, Phys. Rev. **90**, 817 (1953).
[2] R. Peterkop, J. Phys. B **4**, 513 (1971); **9**, L283 (1976); **16**, L387 (1983).
[3] A. R. P. Rau, Phys. Rev. A **4**, 207 (1971).
[4] H. Klar, Z. Phys. A **307**, 75 (1982).
[5] J. M. Feagin, J. Phys. B **17**, 2433 (1984).
[6] S. Cvejanovic and F. H. Read, J. Phys. B **7**, 1841 (1974).
[7] F. Pichou, A. Huetz, G. Joyez, and M. Landau, J. Phys. B **11**, 3683 (1978).
[8] J. Mazeau, A. Huetz, and P. Selles, in *Electronic and Atomic Collisions: Invited Papers of the 14th ICPEAC, 1985,* edited by D. C. Lorents, W. E. Meyerhof, and J. R. Peterson (North-Holland, Amsterdam, 1986), p. 141.
[9] F. H. Read, in *Electron Impact Ionization,* edited by T. D. Mark and G. H. Dunn (Springer-Verlag, New York, 1985), p. 42, and references therein.
[10] J. Mazeau, P. Selles, D. Waymel, and A. Huetz, Phys. Rev. Lett. **67**, 820 (1991).
[11] D. L. Montgomery and D. H. Jaecks, Phys. Rev. Lett. **51**, 1862 (1983).
[12] O. Yenen, D. H. Jaecks, and L. M. Wiese, Phys. Rev. A **39**, 1767 (1989).
[13] O. Yenen, L. M. Wiese, D. Calabrese, and D. H. Jaecks, Phys. Rev. A **42**, 324 (1990).
[14] R. H. McKnight and D. H. Jaecks, Phys. Rev. A **4**, 2281 (1971).
[15] K. Volk, M. Sarstedt, H. Klein, and A. Schempp, Rev. Sci. Instrum. **61**, 493 (1990).
[16] D. H. Jaecks, O. Yenen, L. M. Wiese, and D. Calabrese, Phys. Rev. A **41**, 5934 (1990).
[17] L. J. Schaad and W. V. Hicks, J. Chem. Phys. **61**, 1934 (1974).
[18] D. Talbi and R. P. Saxon, J. Chem. Phys. **89**, 2235 (1989).
[19] H. Weyl, *The Theory of Groups and Quantum Mechanics* (Dover, New York, 1956).
[20] S. Huzinaga, J. Chem. Phys. **42**, 1293 (1965).
[21] G. A. Gallup, J. Chem. Phys. **45**, 2304 (1966).